

# Dissociative recombination of protonated methanol

W. D. Geppert,<sup>\*a</sup> M. Hamberg,<sup>a</sup> R. D. Thomas,<sup>a</sup> F. Österdahl,<sup>b</sup> F. Hellberg,<sup>a</sup>  
V. Zhaunerchyk,<sup>a</sup> A. Ehlerding,<sup>a</sup> T. J. Millar,<sup>c</sup> H. Roberts,<sup>c</sup> J. Semaniak,<sup>d</sup>  
M. af Ugglas,<sup>a</sup> A. Källberg,<sup>e</sup> A. Simonsson,<sup>e</sup> M. Kaminska<sup>d</sup> and M. Larsson<sup>a</sup>

Received 11th November 2005, Accepted 8th February 2006

First published as an Advance Article on the web 19th May 2006

DOI: 10.1039/b516010c

The branching ratios of the different reaction pathways and the overall rate coefficients of the dissociative recombination reactions of  $\text{CH}_3\text{OH}_2^+$  and  $\text{CD}_3\text{OD}_2^+$  have been measured at the CRYRING storage ring located in Stockholm, Sweden. Analysis of the data yielded the result that formation of methanol or deuterated methanol accounted for only 3 and 6% of the total rate in  $\text{CH}_3\text{OH}_2^+$  and  $\text{CD}_3\text{OD}_2^+$ , respectively. Dissociative recombination of both isotopomers mainly involves fragmentation of the C–O bond, the major process being the three-body break-up forming  $\text{CH}_3$ , OH and H ( $\text{CD}_3$ , OD and D). The overall cross sections are best fitted by  $\sigma = 1.2 \pm 0.1 \times 10^{-15} E^{-1.15 \pm 0.02} \text{ cm}^2$  and  $\sigma = 9.6 \pm 0.9 \times 10^{-16} E^{-1.20 \pm 0.02} \text{ cm}^2$  for  $\text{CH}_3\text{OH}_2^+$  and  $\text{CD}_3\text{OD}_2^+$ , respectively. From these values thermal reaction rate coefficients of  $k(T) = 8.9 \pm 0.9 \times 10^{-7} (T/300)^{-0.59 \pm 0.02} \text{ cm}^3 \text{ s}^{-1}$  ( $\text{CH}_3\text{OH}_2^+$ ) and  $k(T) = 9.1 \pm 0.9 \times 10^{-7} (T/300)^{-0.63 \pm 0.02} \text{ cm}^3 \text{ s}^{-1}$  ( $\text{CD}_3\text{OD}_2^+$ ) can be calculated. A non-negligible formation of interstellar methanol by the previously proposed mechanism *via* radiative association of  $\text{CH}_3^+$  and  $\text{H}_2\text{O}$  and subsequent dissociative recombination of the resulting  $\text{CH}_3\text{OH}_2^+$  ion to yield methanol and hydrogen atoms is therefore very unlikely.

## Introduction

Amongst the 125 circumstellar and interstellar molecules hitherto detected,<sup>1</sup> methanol must be counted amongst the most interesting. It has been identified in dark clouds,<sup>2</sup> bipolar outflows,<sup>3</sup> low mass protostars,<sup>4</sup> massive star-forming regions,<sup>5</sup> cometary comae<sup>6</sup> and even in extragalactic sources.<sup>7</sup> Masers of methanol have been described as excellent tracers of star formation.<sup>8</sup> Furthermore, the compound can be used as an evolution indicator during the embedded phase of massive star formation.<sup>9</sup> In star-forming regions, methanol is enhanced by a factor of  $10^2$ – $10^3$  and can undergo a multitude of different chemical processes leading to more complex molecules such as dimethyl ether, methylformate and acetaldehyde.<sup>10</sup>

Since methanol is a slightly asymmetric rotor, ratios between different special lines of the molecule are sensitive to both kinetic temperature and spatial density. Therefore, multi-line observation on methanol can be used to determine these two parameters in an interstellar cloud with one molecule only, thereby avoiding the problem of different spatial distributions of different tracers.<sup>11</sup>

Despite the ample occurrence of methanol and the abundance of information gained by observations of this species, its interstellar formation has so far remained elusive. Although processes on grain surfaces and in grain mantles have been discussed,<sup>12–14</sup> a two step gas phase mechanism involving the radiative association of  $\text{CH}_3^+$  and  $\text{H}_2\text{O}$  with subsequent dissociative

<sup>a</sup> Molecular Physics Division, Department of Physics, Stockholm, Sweden. E-mail: wgeppert@physto.se;

Fax: +46-(0)8-5537 8601; Tel: +46-(0)8-5537 8649

<sup>b</sup> Institute of Physics, Royal Institute of Technology, AlbaNova, SE 10691, Stockholm, Sweden

<sup>c</sup> Institute of Physics, Świętokrzyska Academy, ul. Świętokrzyska 15, PL-25406, Kielce, Poland

<sup>d</sup> Astrophysics Group, School of Physics and Astronomy, University of Manchester, Sackville St. Building, PO Box 88, Manchester, UK M60 1QD

<sup>e</sup> Manne Siegbahn Laboratory, Frescativägen 24, SE-104 05, Stockholm, Sweden

recombination (DR) of the resulting  $\text{CH}_3\text{OH}_2^+$  ion has been thought to be responsible for interstellar methanol production

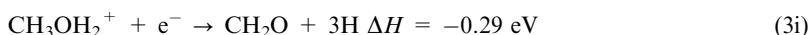
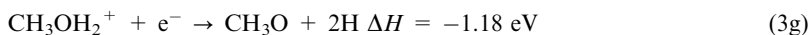
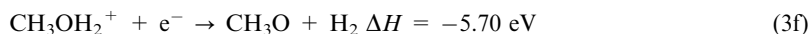
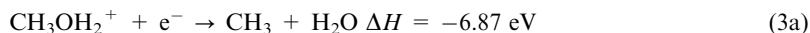


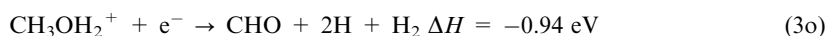
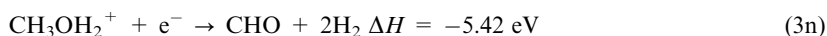
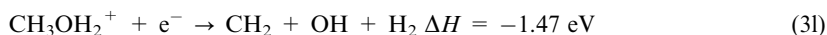
Radiative association reactions normally have rate coefficients that are too low to successfully compete with other interstellar ion processes. However, it can be argued that in more complicated systems the radiative lifetime of the excited adduct could be on the same scale as its dissociative lifetime. Such behaviour has been observed for  $\text{C}_3\text{H}^+$  and  $\text{H}_2$ .<sup>15</sup> Therefore, radiative recombination cannot be ruled out of playing an important role in the formation of stable ions. For larger molecules, it was predicted that the rate coefficients of radiative recombination could be collisionally controlled and exceed  $10^{-9} \text{ cm}^3 \text{ s}^{-1}$ .<sup>16</sup> To reconcile the predictions of the models with the actually observed interstellar abundances, a rate coefficient between  $8 \times 10^{-12} \text{ cm}^3 \text{ s}^{-1}$  and  $8 \times 10^{-8} \text{ cm}^3 \text{ s}^{-1}$  at interstellar temperatures has to be assumed for reaction (1).<sup>17</sup> In an earlier SIFT experiment, a radiative association reaction rate coefficient of  $2 \times 10^{-10} \text{ cm}^3 \text{ s}^{-1}$  has been obtained at 300 K, which would be in accordance with the above-mentioned assumption.

In a recent ion trap experiment a considerably lower upper limit of the rate coefficient ( $2 \times 10^{-12} \text{ cm}^3 \text{ s}^{-1}$ ) was measured for reaction (1).<sup>18</sup> Such a rate coefficient would be at least a factor of 10 too low to explain the observed methanol abundances if one applies the common astrochemical models.<sup>18,19</sup> However, there are several problems with this reasoning. The interstellar abundance of  $\text{CH}_3^+$  has never been measured and has therefore to be taken from model predictions, which could differ considerably from the actual densities. Another source of error might be the interstellar abundance of water. Therefore, concluding only from the new results on reaction (1), the proposed gas phase mechanism for methanol production cannot be ruled out if the DR of  $\text{CH}_3\text{OH}_2^+$  mainly leads to methanol and atomic hydrogen (reaction (2)). Such a propensity should be in line with the theory for the DR reaction formulated by Bates, according to which the reaction pathways involving the least rearrangement of valence bonds should be favoured.<sup>20</sup> This assumption proved unfounded in quite a few DR reactions and reaction pathways regarded as improbable by Bates are, in fact, not uncommon.<sup>21</sup> Especially with larger ions like  $\text{CH}_3\text{OH}_2^+$ , the potential surfaces of the neutral intermediate involved can be very complicated, giving rise to products that are not expected applying chemical "common sense". To finally determine the feasibility of the proposed reaction sequence, both the reaction rate coefficient and branching ratios of the DR of  $\text{CH}_3\text{OH}_2^+$  have to be determined.

Methanol production is, however, not the only point of interest in the DR of  $\text{CH}_3\text{OH}_2^+$ . The ratio of protonated to unprotonated methanol has been used to determine the electron temperature in the inner coma of comet Halley, thereby using the fact that DR is the only process of destruction of  $\text{CH}_3\text{OH}_2^+$  in this environment.<sup>22</sup> Since the square of its rate coefficient serves as input in the formula for determination of the electron temperature, even slight variations in its value might affect the obtained temperature.

Due to the low kinetic energies prevalent in the interstellar medium, only exoergic or very slightly endoergic DR pathways are possible. For  $\text{CH}_3\text{OH}_2^+$  these are the following:





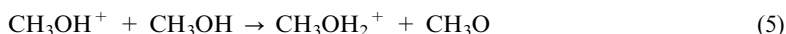
This Discussion contribution presents the determination of the rate coefficient and the branching ratios of the DR of  $\text{CH}_3\text{OH}_2^+$  as well as  $\text{CD}_3\text{OD}_2^+$  at relative kinetic energies resembling those encountered in dark interstellar clouds.

## Experimental

The DR experiments have been performed at the heavy-ion storage ring CRYRING at the Manne Siegbahn Laboratory, Stockholm University. The experimental procedure has been described in detail elsewhere<sup>23</sup> and is therefore summarised only briefly here. For technical reasons related to the data analysis (better resolution on the detector using deuterated compounds)  $\text{CD}_3\text{OD}_2^+$  was also used in the present experiment (see below). The ions were produced in a hollow cathode pulsed discharge ion source (voltage 1–2 kV) from a mixture of (deuterated) methanol and excess hydrogen (deuterium) by the following process through  $\text{H}_3^+$  and  $\text{D}_3^+$ :



It should be mentioned that methanol cations tend to protonate neutral methanol quite efficiently, probably through the following reaction:



which is exoergic by  $61.2 \text{ kJ mol}^{-1}$ .<sup>24</sup> This led to much stronger  $\text{CH}_3\text{OH}_2^+$  than  $\text{CH}_3\text{OH}^+$  mass signals (often by a factor of 5 or more) obtained from our source. Reaction (5) probably proceeds over small clusters of protonated methanol, which have been found to be preferentially formed in methanol–noble gas mixtures by electron impact ionisation.<sup>25</sup> Due to the large intensity of the  $\text{CH}_3\text{OH}_2^+$  signal relative to that of  $\text{CH}_3\text{OH}^+$ , contaminations from  $^{13}\text{CH}_3\text{OH}^+$  or  $\text{CH}_3\text{OD}^+$ , which possess the same mass as  $\text{CH}_3\text{OH}_2^+$  are very unlikely. The same applies for  $\text{CD}_3\text{OD}_2^+$ , which could be contaminated by  $\text{CD}_3^{18}\text{OD}^+$ .

After extraction of the ions from the source at 40 keV, they were mass selected, injected into the ring and accelerated to 2.90 MeV ( $\text{CH}_3\text{OH}_2^+$ ) and 2.53 MeV ( $\text{CD}_3\text{OD}_2^+$ ) translational energy. The stored ion beam was merged with a mono-energetic electron beam in an electron cooler, the length of the interaction region being 0.85 m. During the first 3 s after acceleration, the electron and ion beams were kept at the same average velocity to allow heat transfer from the ion to the electron beam in order to reduce the translational temperature of the ions which then results in an increase of their phase-space density. Furthermore, such storage time enables radiative vibrational cooling of the ions, which might have been formed in a rovibrationally excited state.

Neutral products generated by DR reactions in the electron cooler left the ring tangentially and were detected by an energy-sensitive silicon surface barrier detector (SBD) with a diameter of 17 mm mounted at a distance of 3.85 m from the centre of the interaction region. A background signal due to neutral products emerging from collisions of the ions with residual gas was also present; this was measured with the relative translational energy between the ions and electrons tuned to 1 eV, where the DR cross section is very low and the measured neutral fragments are

therefore almost exclusively produced by rest gas collisions. This background was subsequently subtracted from the total SBD signal.

## Results

### Reaction cross section

During cross section measurements, the relative translational energy between the ions and the electrons was steplessly varied between 1 and 0 eV. This was achieved by changing the cathode voltage of the electron cooler over 1 s from a high value corresponding to a centre-of-mass energy of 1 eV, the electrons being faster than the ions, down to a low value also corresponding to 1 eV where the electrons were slower than the ions. Thus, a voltage corresponding to a centre-of-mass energy of 0 eV is reached during the scan. Before the measurement was started, 3 s of cooling, with the electrons tuned to 0 eV collision energy, was carried out. The signal from the SBD was monitored by a single channel analyser, selecting signals only when all of the fragments reach the detector simultaneously and thereafter recorded by a multichannel scaler, yielding the number of counts *vs.* storage time and, therefore, at a given relative translational collision energy. The experimental DR rate coefficient in the electron cooler is expressed by the formula

$$\langle v_{\text{cm}}\sigma \rangle = \left( \frac{dN}{dt} \right) \frac{v_i v_e e^2 r_e^2 \pi}{I_e I_i l} \quad (6)$$

where  $dN/dt$  is the count rate,  $v_i$  and  $v_e$  are the electron and ion velocities, respectively,  $r_e$  is the radius of the electron beam,  $l$  the length of the interaction region, and  $I_e$  and  $I_i$  are the electron and ion current, respectively. The absolute ion beam current was measured using a Bergoz beam charge monitor with continuous averaging (BCM-CA) and an integrating current transformer in combination with a neutral particle detector installed at the end of one of the straight sections of the ring. Simultaneously with the measurement of the DR count rate, a signal of the ion current was monitored to normalise the DR measurement to it.<sup>26</sup>

The following corrections to the measured data had to be performed: (a) the voltage of the electron cooler cathode (and therefore  $v_e$ ) had to be corrected for space charge effects. (b) The measured rate coefficient  $\langle \sigma v_{\text{cm}} \rangle$  had to be adjusted because of the toroidal effect.<sup>27</sup> The toroidal effect arises from the zones at both ends of the interaction region where the electron beam is bent into or out of the ion beam. In these regions, the transversal electron velocity is higher than in the merged interaction region leading to larger collision energies. (c) The electron beam has (in contrast to the ion beam) a non-negligible energy spread, and the measured reaction rate  $\langle \sigma v_{\text{cm}} \rangle$  has to be deconvoluted according to the formula:

$$\langle v_{\text{cm}}\sigma \rangle = \int_{-\infty}^{\infty} v_e f(v_e) \sigma(v_e) d^3 v_e \quad (7)$$

where  $f(v_e)$  is the velocity distribution. (d) Drag force effects<sup>28</sup> were neglected due to the relatively large mass of the investigated ion. From the resulting cross section constants, the (comparatively) very small contribution to the data due to charge transfer processes with the rest gas had to be subtracted. Since the cross section of the DR is very low at 1 eV collision energy, and the rest gas collisions are independent of the electron velocity, the neutral particles measured at this energy were assumed to be due solely to charge transfer. The obtained final cross sections for  $\text{CD}_3\text{OD}_2^+$ , as functions of the collision energy, are presented in Fig. 1a and 1b. These data are best fitted by the expressions  $\sigma = 1.2 \pm 0.1 \times 10^{-15} E^{-1.15 \pm 0.02} \text{ cm}^2$  and  $\sigma = 9.6 \pm 0.9 \times 10^{-16} E^{-1.20 \pm 0.02} \text{ cm}^2$  for  $\text{CH}_3\text{OH}_2^+$  and  $\text{CD}_3\text{OD}_2^+$ , respectively. The errors from the rate include errors from the current uncertainty of the ion current measurement (about 5%) as well as statistical errors from the data analysis. The total errors can be estimated to be 10%. The thermal reaction rate coefficient can be deduced from the cross sections applying the following formula:

$$k(T) = \frac{8\pi m_e}{(2\pi m_e kT)^{3/2}} \int_0^{+\infty} E \sigma(E) e^{-\frac{E}{kT}} dE \quad (8)$$

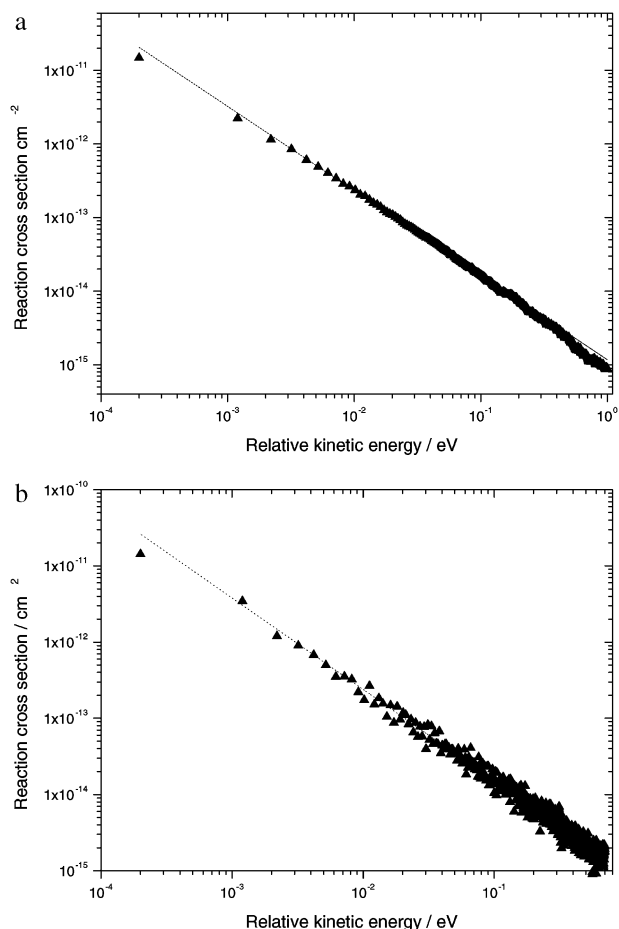


**Fig. 1** (a) Cross section of the DR of  $\text{CH}_3\text{OH}_2^+$ . The dashed line shows the best fit with  $1.2 \pm 0.1 \times 10^{-15} E^{-1.15 \pm 0.02} \text{ cm}^2 \text{ cm}^2$ . (b) Cross section of the DR of  $\text{CD}_3\text{OD}_2^+$ . The dashed line shows the best fit with  $\sigma = 9.6 \pm 0.9 \times 10^{-16} E^{-1.20 \pm 0.02} \text{ cm}^2$ .

where  $m_e$  is the mass of the electron. The temperature dependence of the rate coefficient can then be fitted by the equation  $k(T) = 8.9 \pm 0.9 \times 10^{-7} (T/300)^{-0.59 \pm 0.02} \text{ cm}^3 \text{ mol}^{-1} \text{ s}^{-1}$  and  $k(T) = 9.1 \pm 0.9 \times 10^{-7} (T/300)^{-0.63 \pm 0.02} \text{ cm}^3 \text{ mol}^{-1} \text{ s}^{-1}$  for  $\text{CH}_3\text{OH}_2^+$  and  $\text{CD}_3\text{OD}_2^+$ , respectively.

### Branching ratios

The fragments produced by a DR event reached the detector within a very short time interval compared with the integration time of the detection system. The pulse height of the SBD signal was therefore proportional to the kinetic energy carried by all of the products of the reaction and therefore the total mass. To measure the branching ratios of the DR channels a metal grid with a transmission  $T = 0.297 \pm 0.015$  was inserted in front of the detector.<sup>23</sup> Particles stopped by the grid did not reach the detector. DR events where one of the fragments hit the grid resulted in a signal whose amplitude was proportional to the sum of the kinetic energies of the fragments passing through the grid. The registered DR spectrum therefore splits into a series of peaks with different energies, the intensities of which can be expressed in terms of the probability of the particles passing the grid and the branching ratios of the reaction. For example, in the DR of  $\text{CH}_3\text{OH}_2^+$  the intensity of the  $\text{CH}_3$  peak emerging from reaction (3a) is proportional to  $T(1 - T)\alpha$ , with  $\alpha$  being the branching ratio of reaction (3a) and  $T(1 - T)$  the probability of only the  $\text{CH}_3$  fragment passing the grid.

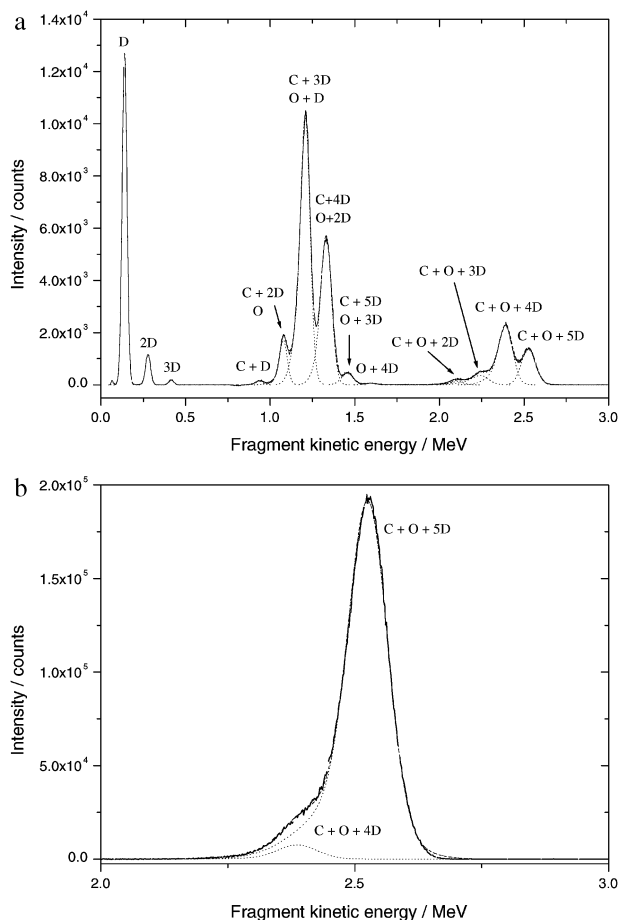


**Fig. 2** (a) Energy spectrum of the neutral fragments of the DR of  $\text{CD}_3\text{OD}_2^+$  (signal from the surface barrier detector) with the grid (transmission = 0.297) in place. The solid line shows the data, whereas the double-Gaussian fitting curves are shown as dashed lines and the total fit as a dotted line. (b) Energy spectrum of the neutral fragments of the DR of  $\text{CD}_3\text{OD}_2^+$  (signal from the surface barrier detector) with the grid (transmission = 0.297) in place. The solid line shows the data, whereas the double-Gaussian fitting curves are shown as dashed lines and the total fit as a dotted line.

The energy spectrum of the DR reaction of  $\text{CD}_3\text{OD}_2^+$  is shown in Fig. 2a. The peaks were fitted to Gaussian functions. As can be seen in Fig. 2a, the final fitting curve is in very good agreement with the data. Concerning the evaluation of the data, two problems arise: firstly, some of the different channels produce products with the same mass distribution and leading to an identical signal distribution in the fragment energy spectrum. This holds for channels (3a) and (3k), and (3c) and (3j) as well as (3l) and (3m). Therefore, there exist three pairs of indistinguishable channels. However, since the formation of  $\text{CD}_4$  would involve a considerable rearrangement of the neutral intermediate, it can be argued that channels (3j) and (3k) are unlikely to play a major role. We will see later that the branching ratio of channels (3l) and (3m) is 0. Furthermore, since there is no signal corresponding to the mass of CO and DCO, channels (3n)–(3q) can be disregarded.

Secondly, owing to the high energy release of reaction (3e), some of the deuterium atoms produced by this pathway might receive a large transversal velocity relative to the propagation direction, and therefore miss the detector. This reduces the contribution of reaction (3e) to the C + O + 5D energy channel to  $T^2(1 - L_e)\epsilon$ , where  $L_e$  is the D-atom loss factor. Conversely, the C + O + 4D energy channel is augmented to  $T(1 - T)(1 - L_e)\epsilon + T\epsilon L_e$ . Analogously, the C + O + 3D channel can be enhanced to  $T(1 - T)(1 - L_\xi)\zeta + T\zeta L_\xi$  by the loss of  $\text{D}_2$  in channel (3f) ( $L_\xi$ ). Using the

$$\begin{pmatrix} I_{(C+O+5D)} \\ I_{(C+O+4D)} \\ I_{(C+O+3D)} \\ I_{(C+O+2D)} \\ I_{(O+4D)} \\ I_{(O+3D,C+5D)} \\ I_{(O+2D,C+4D)} \\ I_{(O+D,C+3D)} \\ I_{(O,C+2D)} \\ I_{(C+D)} \\ I_{(3D)} \\ I_{(2D)} \\ I_{(D)} \end{pmatrix} = \begin{pmatrix} T^2 & T^3 & T^3 & T^3 & T^2(1-L_e) & T^2(1-L_\xi) & T^3 & T^3 & T^4 & T^3 \\ 0 & T^2(1-T) & T^2(1-T) & 0 & T(1-T)(1-L_e)+TL_e & 0 & 2T^2(1-T) & T^2(1-T) & 3T^3(1-T) & 0 \\ 0 & 0 & 0 & T^2(1-T) & 0 & T(1-T)(1-L_\xi)+TL_\xi & T(1-T)^2 & T^2(1-T) & 3T^2(1-T)^2 & T^2(1-T) \\ 0 & 0 & 0 & 0 & 0 & 0 & 0 & T(1-T)^2 & T(1-T)^3 & 0 \\ 0 & 0 & 0 & T^2(1-T) & 0 & 0 & 0 & 0 & 0 & 0 \\ 0 & 0 & T^2(1-T) & 0 & 0 & 0 & 0 & 0 & 0 & T^2(1-T) \\ T(1-T) & 2T^2(1-T) & T(1-T)^2 & T(1-T)^2 & 0 & 0 & 0 & 0 & 0 & T^2(1-T) \\ T(1-T) & 2T(1-T)^2 & T(1-T)^2 & T(1-T)^2 & 0 & 0 & 0 & 0 & 0 & T(1-T)^2 \\ 0 & 0 & T(1-T)^2 & 0 & 0 & 0 & 0 & 0 & 0 & 0 \\ 0 & 0 & 0 & T(1-T)^2 & 0 & 0 & 0 & 0 & 0 & 0 \\ 0 & 0 & 0 & 0 & 0 & 0 & T^2(1-T) & T^3(1-T) & 0 & 0 \\ 0 & 0 & 0 & T(1-T)^2 & 0 & T(1-T)(1-L_\xi) & T^2(1-T) & T(1-T)^2 & 3T^2(1-T)^2 & T(1-T)^2 \\ 0 & T(1-T)^2 & T(1-T)^2 & 0 & T(1-T)(1-L_e) & 0 & 2T(1-T)^2 & T(1-T)^2 & 3T(1-T)^3 & 0 \end{pmatrix} \begin{pmatrix} \alpha \\ \beta \\ \gamma \\ \delta \\ \epsilon \\ \zeta \\ \theta \\ \eta \\ \iota \\ \kappa \end{pmatrix}$$

**Fig. 3** Evaluation matrix for the branching ratios of the DR of  $CD_3OD_2^+$ . The symbols  $\alpha$ ,  $\beta$ ,  $\gamma$  and so on denote the branching ratios of channel (3a), (3b), (3c) and so on.  $L_e$  and  $L_\xi$  are the losses in channel (3e) and (3f), respectively.

transmission probabilities mentioned above, the matrix equation shown in Fig. 3 is formulated for the relative intensities of the different energy (mass) channels.

To evaluate the loss of the deuterium atoms an energy spectrum was measured with the grid removed, and this is depicted in Fig. 2b. Since for this case  $T = 1$  and the sum of all branching ratios equals 1, it can easily be worked out from the above matrix that the ratio between the C + O + 5D peak and the C + O + 4D peak will be

$$I_{C+O+4D}/I_{C+O+5D} = \epsilon L_e / (1 - \epsilon L_e) \quad (9)$$

where  $L_e$  is the loss in channel (3e). Since no signal is found for the C + O + 3D mass in the spectrum with the grid removed,  $L_\xi$  can be concluded to be 0.

By iteratively solving the matrix with a certain loss and evaluating  $L_e$  according to eqn (9), the loss of D-atoms,  $L_e$ , was determined to be  $0.57 \pm 0.05$ . Finally, solving this over-defined matrix with 4 different equations for 3 variables (2 pairs of equations are identical) using a least squares fit leads to the branching ratios listed in Table 1. Since the branching ratio of channel 3e is very small, the error stemming from the loss is negligible.

In order to compare the DR of  $CH_3OH_2^+$  and  $CD_3OD_2^+$  at DR and to elucidate to what extent channels (3j) and (3k), which are indistinguishable from (3b) and (3a), respectively, contribute to the branching ratio of protonated methanol, the branching ratio of  $CH_3OH_2^+$  was also measured.

The fragment kinetic energy spectrum is shown in Fig. 4a. Due to the lighter weight of hydrogen, the velocity of hydrogen atoms produced by reactions (3b)–(3e) will generally be larger and hydrogen loss can be expected from these channels. Also, losses of  $H_2$  from pathways (3f) and (3h) are possible. Fig. 4b, which depicts the spectrum with the grid removed, clearly shows a contribution of the C + O + 3H signal. It is impossible to estimate all the contributions of the different channels to the H or  $H_2$  losses. To be able to evaluate the fragment energy spectrum one has to make three different assumptions: Firstly, we postulate that the kinetic energy release in

**Table 1** Branching ratios of the DR of  $CD_3OD_2^+$

Reaction channel	Products	Branching ratio
3a (3k)	$CD_3 + D_2O$ ( $CD_4 + OD$ )	$0.11 \pm 0.02$
3b	$CD_3 + DO + D$	$0.59 \pm 0.04$
3c (3j)	$CD_2 + D + D_2O$	$0.17 \pm 0.02$
3d	$CD + D_2 + D_2O$	$0.01 \pm 0.01$
3e	$CD_3OD + D$	$0.06 \pm 0.02$
3f	$CD_3O + D_2$	$0.05 \pm 0.02$
3g	$CD_3O + 2D$	$0.00 \pm 0.01$
3h	$CD_2O + D_2 + D$	$0.02 \pm 0.01$

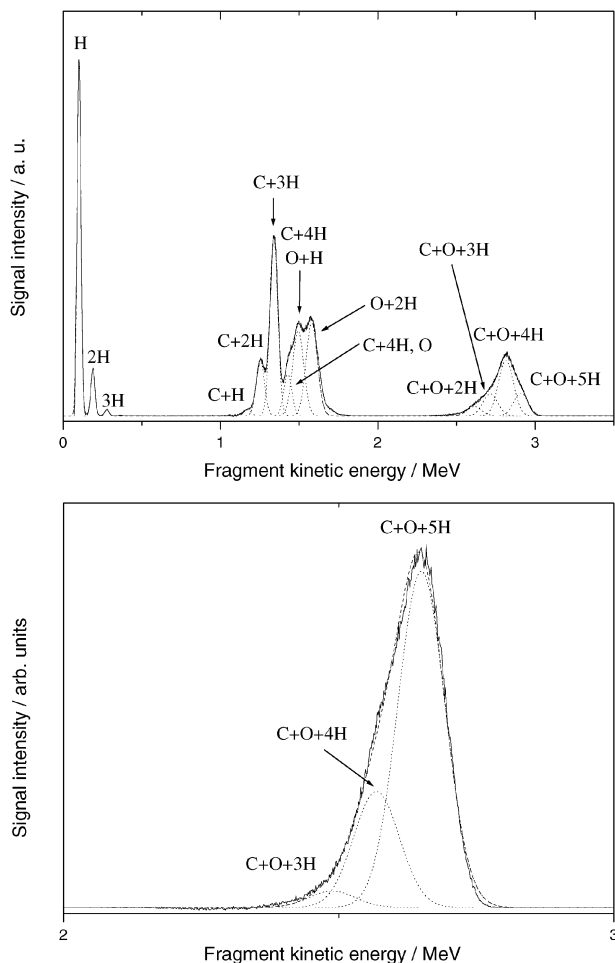


**Fig. 4** (a) Energy spectrum of the neutral fragments of the DR of  $\text{CH}_3\text{OH}_2^+$  (signal from the surface barrier detector) with the grid (transmission = 0.297) in place. The solid line shows the data, whereas the double-Gaussian fitting curves are shown as dashed lines and the total fit as a dotted line. (b) Energy spectrum of the neutral fragments of the DR of  $\text{CH}_3\text{OH}_2^+$  (signal from the surface barrier detector) with the grid removed. The solid line shows the data, whereas the double-Gaussian fitting curves are shown as dashed lines and the total fit as a dotted line.

channel (3e) is the same for the DR of  $\text{CH}_3\text{OH}_2^+$  and  $\text{CD}_3\text{OD}_2^+$ . Assuming an isotropic distribution of the fragments, the kinetic energy release leading to the observed D loss from channel (3e) of the DR of  $\text{CD}_3\text{OD}_2^+$  (0.56) is 3.45 eV. The same energy release would lead to a H loss of 0.73 in the analogous reaction pathway with  $\text{CH}_3\text{OH}_2^+$ . Secondly, since channels (3b) and (3c) are the most dominant H-producing channels it is expected that the rest of the observed H loss is due to these pathways. It is further expected that in these two pathways a similar fraction of the total reactive energy is converted into kinetic energy. This assumption is, admittedly, somewhat crude, but since we are not able to gauge the exact contribution of each of these channels it is necessary. Thirdly, we estimate that the loss of  $\text{H}_2$  is mostly due to reaction (3f), because it is the major pathway producing mass 2 and is highly exoergic. The ratio of the C + O + 4H to the C + O + 5H peak in the spectrum without the grid then becomes:

$$I_{\text{C+O+4H}}/I_{\text{C+O+5H}} = (\varepsilon L_\varepsilon + \beta L_\beta + \gamma L_\gamma) / (1 - \varepsilon L_\varepsilon - \beta L_\beta - \gamma L_\gamma - \xi L_\xi) \quad (10)$$



find a somewhat greater propensity of  $\text{CH}_3\text{OH}_2^+$  (0.82) to undergo such processes compared with  $\text{H}_3\text{O}^+$  (0.61<sup>29</sup> and 0.71,<sup>23</sup> respectively). This might be due to the higher number of three-body producing channels available in the DR of  $\text{CH}_3\text{OH}_2^+$ .

It is also interesting to compare the behaviour of the undeuterated with the deuterated ion. Apart from a fairly moderate enhancement of the branching ratios of channels (3b) and (3c) and a reduction in the case of channels (3h) no significant changes are observed. This is similar to the findings with  $\text{H}_3\text{O}^+$  and  $\text{D}_3\text{O}^+$ .<sup>23,29</sup> Also, the overall branching ratio of three-body channels (0.82 for  $\text{CH}_3\text{OH}_2^+$  and 0.78 for  $\text{CD}_3\text{OD}_2^+$ ) only changes slightly upon deuteration.

Since performing imaging is impossible due to the large number of different channels and the possibility of the production of vibrationally excited states in the products, one can only speculate about the mechanism of the DR reaction. It is, however, not unlikely that the following sequential two step mechanism happens: first, a hydrogen atom is released from the neutral intermediate. Only in the case of high kinetic energy release does the methanol fragment not undergo subsequent reactions. This is in line with the relatively large kinetic energy release (3.45 eV) concluded from the D loss in channel (3e) in the DR of  $\text{CD}_3\text{OD}_2^+$ . If there is sufficient energy, the methanol fragment further breaks up into smaller parts. This is corroborated by the fact that in channels (3b) and (3c) high kinetic energy releases are also obtained, which points to formation of the final product in a low vibrational state. The energy gained by the initial recombination step is therefore likely to be stored in vibrational modes that are prone to dissociation (e.g. the C–O stretch). One exception of this might be the OH-stretching vibration since channel (3g), which leads to  $\text{CH}_3\text{O} + 2\text{H}$ , is absent. Generally, one interesting feature is the lack of importance of pathways producing the comparatively stable  $\text{CH}_3\text{O}$  ( $\text{CD}_3\text{O}$ ) radical, but no simple explanation for this springs to mind.

Reaction rate coefficients are very similar in  $\text{CD}_3\text{OD}_2^+$  and  $\text{CH}_3\text{OH}_2^+$ . In  $\text{H}_3\text{O}^+$ , no large changes of the rate coefficient have been found upon deuteration by Jensen *et al.*<sup>29</sup> Interestingly, the CRYRING experiment yielded a DR rate coefficient at 300 K which was more than a factor of 2 lower in  $\text{D}_3\text{O}^+$  compared with that obtained for  $\text{H}_3\text{O}^+$ . Generally, the DR rate coefficients of  $\text{CD}_3\text{OD}_2^+$  and  $\text{CH}_3\text{OH}_2^+$  found in this study are about a factor of two higher than those measured for  $\text{H}_3\text{O}^+$  ( $\text{D}_3\text{O}^+$ ). They are, however, in excellent agreement with the value of  $8.8 \times 10^{-7} \text{ cm}^3 \text{ s}^{-1}$  obtained for  $\text{CH}_3\text{OH}_2^+$  in an earlier afterglow experiment.<sup>33</sup>

## Astrophysical implications

Branching ratios for the DR of interstellar ions have long been found to affect greatly the predictions of gas phase models of dark interstellar clouds.<sup>34</sup> This holds especially for methanol, where the mere possibility of gas phase production might be challenged by unexpected branching ratios in the DR of  $\text{CH}_3\text{OH}_2^+$ . Therefore, the new data on the rate coefficient and the branching ratios on DR of  $\text{CD}_3\text{OD}_2^+$  was used as an input for a model calculation of a dark cloud resembling TMC-1 using the UMIST code.<sup>35</sup> The branching ratios of the deuterated isotopomer were used because of the higher certainty of the data due to the lower presence of detection losses of light particles. Using the old data, the model predicted a methanol peak abundance relative to  $\text{H}_2$  of  $1 \times 10^{-9}$ , which is in good agreement with the observations of Friberg *et al.*,<sup>36</sup> which yielded a methanol abundance in the low digits of  $10^{-9}$  for TMC-1.<sup>2,35</sup> With the present rate coefficient and branching ratios of the DR of protonated methanol, the peak abundance is lowered to a value of  $8 \times 10^{-11}$  while that for the steady state sinks from  $3 \times 10^{-10}$  to  $2 \times 10^{-11}$ . If the recently measured rate coefficient for the radiative association of  $\text{CH}_3^+$  and  $\text{H}_2\text{O}$ <sup>18</sup> is also included, the peak abundance is further diminished to  $7 \times 10^{-13}$  and the steady state to  $1 \times 10^{-13}$ , which is definitely below the observed values in dark clouds and probably below the detection limits for existing telescopes (see Fig. 6). When these two new findings are put together, they clearly provide the final nail in the coffin for the proposed chemical gas phase production of methanol.

Therefore, the question of alternative mechanisms for interstellar methanol production arises. Photoproduction in grain mantles have been discussed but although some models including such processes could produce adequate  $\text{CH}_2\text{O} : \text{H}_2\text{O}$  ratios,<sup>37</sup> they fail to explain the observed methanol abundances.<sup>13</sup> Formation of methanol on grain surfaces has also long been discussed.<sup>14</sup> There are, however, two problems with this supposition. Firstly, it is difficult to imagine how methanol is formed on grain surfaces given the very low temperatures prevailing in dark clouds. Secondly, there must be a

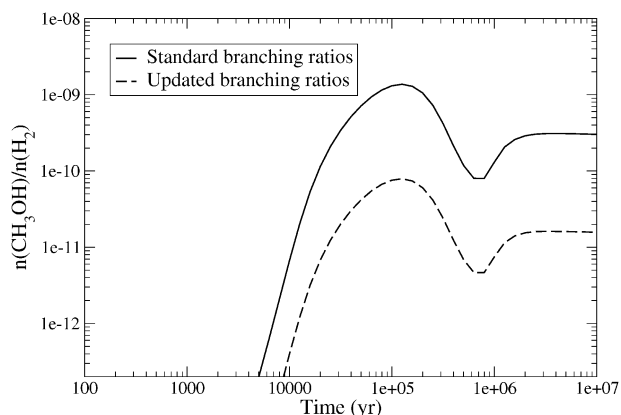


**Fig. 6** Model calculations using the unchanged reaction rate coefficients from the new UMIST database from 1999 (solid line) and with the DR branching rates and the rate coefficient from the present paper (dashed line).

mechanism to release methanol formed on grains into the gas phase, which is also not easy to accomplish under these conditions, since the desorption energy of methanol is comparatively high.<sup>38</sup>

Gas-grain models have included repetitive hydrogenation of CO leading to methanol.<sup>39</sup> Unfortunately, two of the steps involved, namely the reactions  $\text{H} + \text{CO} \rightarrow \text{HCO}$  and  $\text{H} + \text{H}_2\text{CO} \rightarrow \text{H}_3\text{CO}$  are not barrierless and exhibit thresholds of 26.4 and 73.6 meV, respectively. Also, clustering with water, which would be an issue in mixed CO–H<sub>2</sub>O ices, does not reduce this barrier significantly.<sup>40</sup> However, very recently it has been established in a surface reaction experiment that the formation of methanol by hydrogenation of CO with H on pure CO and mixed CO–H<sub>2</sub>O ices proceeds efficiently at 10 K. Moreover, once produced, CH<sub>3</sub>OH is not degraded by irradiation, making CO hydrogenation a feasible pathway for methanol production in dark interstellar clouds.<sup>41</sup> This is also in line with recent observations where a high degree of correlation between CO and methanol abundances has been found in star-forming regions.<sup>42</sup> Furthermore, deuterium fractionation observed with methanol indicates a grain surface process for its production.<sup>43</sup>

The question remains as to how methanol produced on surfaces can desorb to a sufficient extent to produce the methanol abundances observed in dark interstellar clouds. Desorption by vibrational excitation could be a possibility. Hydrogenation of the precursor methoxy or hydroxymethyl radicals is highly exoergic ( $\Delta H = -4.51$  and  $-4.07$  eV, respectively)<sup>24</sup> and might lead to methanol in a highly excited vibrational state. The resulting methanol molecule might use a part of this energy to recoil from the surface and thus end up in the gas phase. The question regarding the extent to which this is possible still lacks a definitive answer.

Very recently, the reaction database used in the UMIST database has been updated. The results for the methanol abundances *vs* cloud age are depicted in Fig. 7. It is interesting to note that the introduction of the new DR rate coefficient of protonated methanol strongly affects the peak abundance of methanol, whereas the rate coefficient for the radiative association of CH<sub>3</sub><sup>+</sup> and H<sub>2</sub>O does not. Also, the maximum of the methanol abundance is shifted. The reason for this different behaviour is that, according to the predictions of the newer model calculations, a new pathway of methanol production opens, involving H<sub>3</sub><sup>+</sup> and acetaldehyde



The rate coefficient for this reaction has been measured in a flowing afterglow experiment and found to be  $1.4 \times 10^{-9} \text{ cm}^3 \text{ s}^{-1}$  at 300 K.<sup>44</sup> If one uses both new rate coefficients for the methanol production mechanism involving radiative association and DR, reaction (12) accounts for 94% of the total methanol formation. On the other hand, the steady state abundances are affected by both the DR and radiative association rate. Including both, the steady state abundance of methanol relative to H<sub>2</sub> is lowered to  $8 \times 10^{-12}$ , which, again, is more than a factor of 100 below the observed values. This casts severe doubts on the feasibility of reaction (12) to produce methanol with the abundances observed in TMC-1.<sup>2</sup>

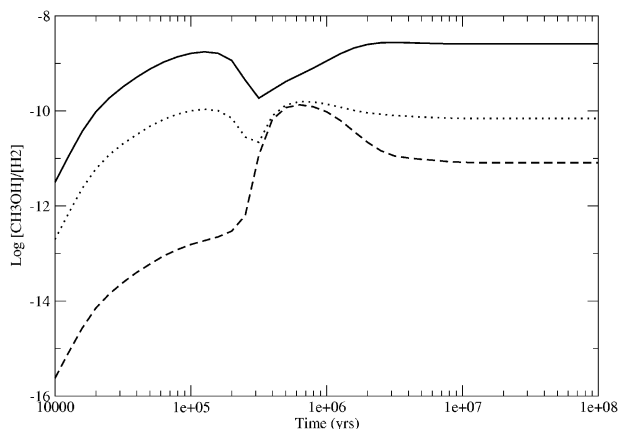


**Fig. 7** Model calculations using the unchanged reaction rate coefficients from the new UMIST database from 2004 (solid line), with the DR branching rates and the rate coefficient from the present paper but with the previously used radiative association rate (dotted line), and with both new rates and branching ratios (dashed line).

Furthermore, there are several problems associated with reaction 12. The rate coefficient has only been measured at 300 K, so conclusions about its temperature dependence cannot be drawn. It cannot even be excluded that the process has, although being exoergic, a small barrier and therefore is unfeasible for dark interstellar clouds. Secondly, the new calculations yield a  $\text{H}_2\text{O}/\text{H}_2$  ratio that is about  $1.4 \times 10^{-5}$  at both peak and steady state, some 100–1000 times larger than observed. This discrepancy could be large enough to seriously damage the validity of these predictions.

As mentioned earlier, the  $\text{CH}_3\text{OH}_2^+ : \text{H}_3\text{O}^+$  ratio was used to determine the electron temperature in the inner coma of comet Halley.<sup>6</sup> The rate coefficient used for the DR of  $\text{CH}_3\text{OH}_2^+$  was a rounded down value compared to the one determined by Adams and Smith,<sup>33</sup> namely  $8 \times 10^{-7} (T/300)^{-0.50} \text{ cm}^3 \text{ s}^{-1}$ .<sup>45</sup> Although DR is predicted to be by far the most dominant process of  $\text{CH}_3\text{OH}_2^+$  in the inner coma (2000–18 000 km from the core) and the DR rate coefficient is included as square into the formula for the electron temperature, a dramatic change of the latter emerging from the slightly higher DR rate coefficient found in our experiment is unlikely.

## Conclusions

In the DR of both  $\text{CH}_3\text{OH}_2^+$  and  $\text{CD}_3\text{OD}_3^+$  the channel leading to H,  $\text{CH}_3$  and OH (or the respective deuterated fragments) is by far the most dominant channel. The pathway leading to (deuterated) methanol and hydrogen (deuterium) atoms has only very low branching ratios for both isotopomers. Generally, only slight to moderate changes of the branching ratios upon deuteration are found. The overall rate coefficients of the reaction are also very similar and follow the equations  $k(T) = 8.9 \pm 0.9 \times 10^{-7} (T/300 \text{ K})^{-0.59 \pm 0.02} \text{ cm}^3 \text{ s}^{-1}$  and  $k(T) = 9.1 \pm 0.9 \times 10^{-7} (T/300 \text{ K})^{-0.63 \pm 0.02} \text{ cm}^3 \text{ s}^{-1}$  for  $\text{CH}_3\text{OH}_2^+$  and  $\text{CD}_3\text{OD}_2^+$ , respectively. Model calculations show that the present findings together with recent measurements of the radiative recombination of  $\text{CH}_3^+$  and  $\text{H}_2\text{O}^{18}$  exclude the possibility of the previously proposed gas phase production of interstellar methanol.

## Acknowledgements

Financial support from the Swedish Space Board and the Swedish Research Council is gratefully acknowledged. W. D. Geppert is indebted to the European Union (EU) for granting a “Marie Curie Individual Fellowship” under the EU programme “Improving Human Potential”, contract number HMPF-CT-200201583. Support from the EU IHP Research Training Network programme under contract HPRN-CT-2000-0142 is also gratefully acknowledged. RDT thanks the Swedish Research Council, for a research fellowship (diary number 2003–2889). J. Semaniak and M. Kamińska are

grateful for partial support by the State Committee for Scientific Research, Poland. Molecular astrophysics at the University of Manchester is supported by a grant from PPARC. The authors also want to thank the staff at Manne Siegbahn Laboratory for excellent technical assistance.

## References

- 1 The 125 interstellar and circumstellar molecules, <http://www.cv.nrao.edu/~awooten/allmols.html>.
- 2 P. Friberg, S. C. Madden, Å. Hjalmarson and W. M. Irvine, *Astron. Astrophys.*, 1988, **195**, 281.
- 3 G. Garay, I. Köhnenkamp, T. L. Bourke, L. F. Rodríguez and K. L. Lehtinen, *Astrophys. J.*, 1998, **509**, 768.
- 4 S. Maret, C. Ceccarelli, A. G. G. M. Tielens, E. Caux, B. Lefloch, A. Faure, A. Castets and D. R. Flower, *Astron. Astrophys.*, 2005, **442**, 527.
- 5 E. C. Sutton, A. M. Sobolev, S. V. Salii, A. M. Malyshec, A. B. Ostrovskii and I. I. Zinchenko, *Astrophys. J.*, 2004, **609**, 231.
- 6 P. Eberhardt, R. Meier, D. Krankowsky and R. R. Hodges, *Astron. Astrophys.*, 1994, **288**, 315.
- 7 C. Henkel, R. Mauersberger, T. Viklund, S. Hüttemeister, C. Lemme and T. J. Millar, *Astron. Astrophys.*, 1993, **268**, L17.
- 8 V. Minier, *Technical Report No. 395*, Chalmers University of Technology, Gothenburg, 2000.
- 9 F. F. S. van der Tak, E. F. van Dishoeck and P. Caselli, *Astron. Astrophys.*, 2000, **361**, 327.
- 10 S. B. Charnley, M. E. Kress, A. G. G. M. Tielens and T. J. Millar, *Astrophys. J.*, 1995, **448**, 232, and references therein.
- 11 S. Leurini, P. Schilke, K. M. Menten, D. R. Flower, J. T. Pottage and L. H. Xu, *Astron. Astrophys.*, 2004, **422**, 573.
- 12 M. Allen and G. W. Robinson, *Astrophys. J.*, 1977, **212**, 396.
- 13 O. M. Schalabica and J. M. Greenberg, *Astron. Astrophys.*, 1994, **290**, 266.
- 14 A. G. G. M. Tielens and L. J. Allamandola, in *Physical Processes in Interstellar Clouds*, ed. G. Morfill and M. Scholer, Dordrecht, Reidel, 1987, p. 233.
- 15 A. Sorgenfrei and D. Gerlich, Ion Trap Experiments on Radiative Association versus Hydrogen Abstraction, in *Physical Chemistry of Molecules and Grains in Space*, ed. I. Nenner, AIP Press, New York, 1994, p. 505.
- 16 E. Herbst and R. C. Dunbar, *Mon. Not. R. Astron. Soc.*, 1991, **253**, 341.
- 17 C. A. Gottlieb, J. A. Ball, E. W. Gottlieb and D. F. Dickinson, *Astrophys. J.*, 1979, **227**, 422.
- 18 A. Luca, D. Voulot and D. Gerlich, *WDS'02 Proceedings of Contributed Papers PART II*, 2002, 294.
- 19 E. Herbst, *Astrophys. J.*, 1985, **291**, 226.
- 20 D. R. Bates, *Astrophys. J. Lett.*, 1986, **306**, 45.
- 21 (a) M. Larsson and R. Thomas, *Phys. Chem. Chem. Phys.*, 2001, **3**, 4471; (b) W. D. Geppert, R. Thomas, A. Ehlerding, J. Semaniak, F. Österdahl, M. af Ugglas, N. Djurić, A. Paál and M. Larsson, *Faraday Discuss.*, 2004, **127**, 425.
- 22 P. Eberhardt and D. Krankowsky, *Astron. Astrophys.*, 1995, **295**, 795.
- 23 A. Neau, A. Al-Khalili, S. Rosén, A. Le Padellec, A. M. Derkatch, W. Shi, L. Viktor, M. Larsson, M. B. Nagard, K. Andersson, H. Danared and M. af Ugglas, *J. Chem. Phys.*, 2000, **113**, 1762.
- 24 S. G. Lias, J. E. Bartmess, J. Liebman, J. L. Holmes, R. D. Levin and W. G. Mallard, *J. Phys. Chem. Ref. Data*, 1988, **17**.
- 25 S. Y. Lee, D. N. Shin, S. G. Cho, K.-H. Jung and K. W. Jung, *J. Mass Spectrom.*, 1995, **30**, 969.
- 26 A. Paál, A. Simonsson, A. Källberg, J. Dietrich and I. Mohos, *EPAC 9th European Particle Conference Particle Accelerator Conference*, Lucerne, 2004, 2745.
- 27 A. Lampert, A. Wolf, D. Habs, J. Kenntner, G. Kilgus, D. Schwalm, M. S. Pindzola and N. R. Badnell, *Phys. Rev. A*, 1996, **53**, 1413.
- 28 H. Danared, G. Andler, L. Bagge, C. J. Herrlander, J. Hilke, J. Jeansson, A. Källberg, A. Nilsson, A. Paál, K.-G. Rensfelt, U. Rosengård, J. Starker and M. af Ugglas, *Phys. Rev. Lett.*, 1994, **73**, 377.
- 29 M. J. Jensen, R. C. Bilodeau, C. P. Safvan, K. Seiersen, L. H. Andersen, H. B. Pedersen and O. Heber, *Astrophys. J.*, 2000, **543**, 764.
- 30 N. G. Adams, C. R. Herd, M. Geoghegan, D. Smith, A. Canosa, J. C. Gomet, B. R. Rowe, J. Le Queffelec and M. Mortais, *J. Chem. Phys.*, 1991, **94**, 4852.
- 31 T. L. Williams, N. G. Adams, L. M. Babcock, C. R. Herd and M. Geoghegan, *Mon. Not. R. Astron. Soc.*, 1996, **282**, 413.
- 32 C. R. Herd, N. G. Adams and D. Smith, *Astrophys. J.*, 1990, **485**, 689.
- 33 N. G. Adams and D. Smith, *Chem. Phys. Lett.*, 1988, **144**, 11.
- 34 T. J. Millar, D. J. De Freed, A. D. McLean and E. Herbst, *Astron. Astrophys.*, 1988, **194**, 250.
- 35 A. Markwick, T. J. Millar and S. B. Charnley, *Astrophys. J.*, 2000, **535**, 256.
- 36 P. Friberg, S. C. Madden, Å. Hjalmarson and W. M. Irvine, *Astron. Astrophys.*, 1988, **195**, 281.
- 37 W. Schutte, P. A. Gerakines, E. F. van Dishoeck, J. M. Greenberg and T. R. Geballe, in *Physical Chemistry of Molecules and Grains In Space*, Mont Sainte Odile, France, 1994.
- 38 T. Stantcheva, V. I. Shematovich and E. Herbst, *Astron. Astrophys.*, 2002, **391**, 1069.

- 
- 39 T. Stantcheva and E. Herbst, *Astron. Astrophys.*, 2004, **423**, 241.  
40 D. E. Woon, *Astrophys. J.*, 2002, **569**, 541.  
41 H. Hidaka, N. Watanabe, T. Shiraki, A. Nagaoka and A. Kouchi, *Astrophys. J.*, 2004, **614**, 1124.  
42 S. E. Bisschop, J. K. Jørgensen and E. F. van Dishoeck, *2005 Proceedings of the IAU Symposium No. 231*, 2005, to be published.  
43 B. Parise, A. Castets, E. Herbst, E. Caux, C. Ceccarelli, I. Mukhopadhyay and A. G. G. M. Tielens, *Astron. Astrophys.*, 2004, **416**, 159.  
44 H. S. Lee, M. Drucker and N. G. Adams, *Int. J. Mass Spectrom. Ion Processes*, 1992, **117**, 101.  
45 P. Eberhardt, R. Meier and D. Krankowski, *Astron. Astrophys.*, 1994, **288**, 315.